Synchro-Waveform State Estimation: Formulation, Closed-Form Solution, and Robustness

Hossein Mohsenzadeh-Yazdi, *Student Member, IEEE*, Mahnoosh Alizadeh, *Senior Member, IEEE*, and Hamed Mohsenian-Rad, *Fellow, IEEE*

***Abstract*—Building on recent advances in smart grid sensor technologies, this paper introduces Synchro-Waveform State Estimation (SWSE), a new time-domain framework that continuously estimates instantaneous voltage and current waveforms across the power network. The SWSE problem is formulated using physics-derived equations, and a closed-form solution is obtained to ensure efficient and scalable computation. To support practical deployment, the paper further proposes a robust algorithm that automatically detects and mitigates data quality issues in waveform measurements, including measurement noise, outliers, latched samples, and time-synchronization errors. Case studies show that the proposed SWSE methods achieve accurate time-domain state estimation even under severe data distortions. The results position SWSE as a strong foundation for next-generation synchro-waveform applications in modern power systems.**

***Keywords*— Synchro-waveform state estimation, WMU, point-on-wave, time-domain estimation, robustness, data quality issues.**

I. Introduction

Over the past decade, Phasor Measurement Units (PMUs) have enhanced state estimation (SE) by providing time-synchronized voltage/current phasors, which have been widely used in transmission system static SE [1], transmission system dynamic SE [2], and distribution system SE [3]. However, the objective of PMU-based SE remains the same as in traditional SE: estimating the *phasor representations* of the fundamental frequency components of bus voltages and line currents [4].

Beyond estimating the fundamental phasors, the broader traditional literature on SE also includes various extensions for Power Quality (PQ) State Estimation, such as harmonic, [5], voltage sag [6], and transient [7] state estimation.

Recently, *synchro-waveform* technologies have emerged in smart grid sensing, providing continuous, high-resolution, time-synchronized voltage and current waveform measurements [8]. These measurements are collected by Waveform Measurement Units (WMUs) [9], which report point-on-wave samples at high rates (e.g., 15.36 kilo-samples per second).

Synchro-waveforms support several emerging applications, such as oscillation analysis [10], fault detection [11], monitoring inverter-based resources [12], and event location [13].

Synchro-waveform State Estimation (SWSE) can play a critical role in supporting the aforementioned applications and other emerging uses of synchro-waveform data by providing a *unified extension* of existing state estimation approaches. By continuously estimating voltage and current waveforms across the network, SWSE enables derivation of fundamental and harmonic phasors, transient distortions, and voltage sags.

H. M. Yazdi and H. Mohsenian-Rad (Corresponding Author) are with UC Riverside, USA. M. Alizadeh is with UC Santa Barbara, USA. This work is supported in part by NSF Grants ECCS 2330155 and ECCS 2330154.

In SWSE, the state variables are the *instantaneous* nodal voltages in the *time domain* across the power network. As a result, the formulation and solution of the SWSE problem are inherently more complex than those of traditional SE.

Furthermore, due to the high-resolution nature of waveform measurements, SWSE is more susceptible and more sensitive to various *data quality challenges*, such as measurement noise affecting individual waveform samples, occasional corruption of sampled data (e.g., erroneous or latched sampling points), and momentary timing errors in sample synchronization.

Motivated by the above challenges and opportunities, this paper presents a novel method to solve the SWSE problem in a manner that is *algorithmically robust* to data quality issues.

II. SWSE Problem Formulation

Consider a power system that is equipped with WMUs; as in Fig. 1. Let $\mathcal{N}$ denote the set of all buses and $\mathcal{L}$ denote the set of all power lines. The vector of all nodal voltage waveforms and all line current waveforms are defined as

$$\mathbf{v}(t) = [v_1(t) \dots v_{n\in\mathcal{N}}(t)]^T, \mathbf{i}(t) = [i_1(t) \dots i_{m\in\mathcal{L}}(t)]^T. \quad (1)$$

Let $\mathbf{z}(t) = [\mathbf{z}_v(t); \mathbf{z}_i(t)]$ denote the vector of all synchro-waveform measurements by all WMUs, including voltage measurements $\mathbf{z}_v(t)$ and current measurements $\mathbf{z}_i(t)$, where

$$\begin{aligned} \mathbf{z}_v(t) &= [\hat{v}_1(t) \ \dots \ \hat{v}_{n\in\mathcal{N}}(t)]^T = \mathbf{v}(t) + \boldsymbol{\varepsilon}_v(t), \\ \mathbf{z}_i(t) &= [\hat{i}_1(t) \ \dots \ \hat{i}_{m\in\mathcal{L}}(t)]^T = \mathbf{i}(t) + \boldsymbol{\varepsilon}_i(t). \end{aligned} \quad (2)$$

Here, $\boldsymbol{\varepsilon}_v(t)$ and $\boldsymbol{\varepsilon}_i(t)$ denote the vectors of measurement errors corresponding voltage and current waveforms, respectively.

We define $\mathbf{x}(t) = \mathbf{v}(t)$ as the vector of state variables in the SWSE problem formulation. From (2), we have:

$$\mathbf{z}_v = \mathbf{x} + \boldsymbol{\varepsilon}_v(t). \quad (3)$$

As for the relationship between $\mathbf{z}_i$ and $\mathbf{x}$, it depends on the network model and its physics-based equations. For example, suppose we model the transmission line between bus a and bus b using the π-equivalent model [14], with inductor L_{ab}, resistor R_{ab}, and line-equivalent capacitor C_a. From Kirchhoff's Voltage Law (KVL), Kirchhoff's Current Law (KCL), Ohm's Law, Faraday's Law, and Gauss's Law, we have:

$$\begin{aligned} v_a(t) - v_b(t) = L_{ab}\,\frac{d}{dt}\left(i_a - C_a\frac{d\,v_a(t)}{dt}\right) + \\ R_{ab}\left(i_a - C_a\frac{d\,v_a(t)}{dt}\right). \end{aligned} \quad (4)$$

The relationship in (4), as well as any other physics-based equation in the power system, can be used to relate $\mathbf{z}_i$ to $\mathbf{x}$.

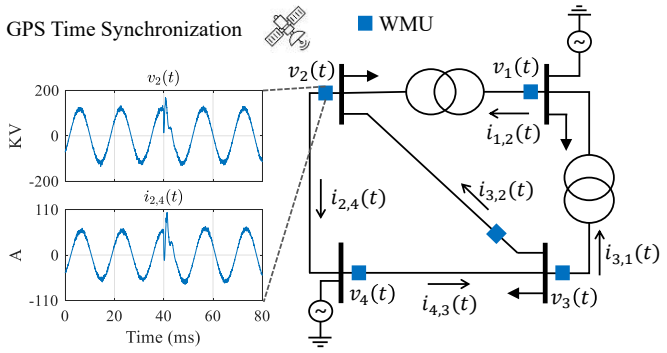

Fig. 1. A power network that is equipped with GPS-synchronized WMUs, measuring high-resolution voltage and current waveforms in time-domain.

Broadly speaking, we can express such relationships in form of *differential equations*, such as in this generic form:

$$\mathbf{A}_2\ddot{\mathbf{x}}(t) + \mathbf{A}_1\dot{\mathbf{x}}(t) + \mathbf{A}_0\mathbf{x}(t) = \mathbf{B}_1\dot{\mathbf{z}}_i(t) + \mathbf{B}_0\mathbf{z}_i(t), \quad (5)$$

where matrices $\mathbf{A}_0$, $\mathbf{A}_1$, $\mathbf{A}_2$, $\mathbf{B}_0$, and $\mathbf{B}_1$ are constructed based on the specific physics-based equations. They are all constants.

Due to the measurement errors, we must rewrite (5) as:

$$\mathbf{B}_1\dot{\mathbf{z}}_i(t)+\mathbf{B}_0\mathbf{z}_i(t) = \mathbf{A}_2\ddot{\mathbf{x}}(t)+\mathbf{A}_1\dot{\mathbf{x}}(t)+\mathbf{A}_0\mathbf{x}(t)+\boldsymbol{\omega}_i(t), \quad (6)$$

where $\boldsymbol{\omega}_i(t) = \mathbf{B}_1\dot{\boldsymbol{\varepsilon}}_i + \mathbf{B}_0\boldsymbol{\varepsilon}_i$; see the definition of $\boldsymbol{\varepsilon}_i$ in (2).

A. Theoretical Continuous-Time Formulation

The equations in (3) and (6) provide the relationships between the measurements $\mathbf{z}_v(t)$ and $\mathbf{z}_i(t)$ and the state variables $\mathbf{x}(t)$. Access to *both* nodal voltage and line current waveforms provides *redundancy* in the measurements, helping mitigate the impact of measurement errors. With this setup, we can formulate the SWSE as the following least-squares problem:

$$\min_{\mathbf{x}(t)} \int_t \Big[\|\mathbf{x}(t) - \mathbf{z}_v(t)\|_2^2 + \lambda\|\mathbf{A}_2\ddot{\mathbf{x}}(t) + \mathbf{A}_1\dot{\mathbf{x}}(t)+ \mathbf{A}_0\mathbf{x}(t) - \mathbf{B}_1\dot{\mathbf{z}}_i(t) - \mathbf{B}_0\mathbf{z}_i(t)\|_2^2\Big] dt. \quad (7)$$

The first term in (7) penalizes deviations from the measured voltage waveforms $z_v(t)$, while the second term enforces consistency with the measured current waveforms $z_i(t)$. Parameter λ balances the trade-off between the two terms.

B. Practical Discrete-Time Formulation

WMUs provide discrete-time point-on-wave measurement samples at fixed sampling rates. Thus, the SWSE problem in (7) must be formulated and solved in the discrete-time domain.

Consider the trapezoidal discretization method:

$$dx(t)/dt \approx (x[k\Delta t] - x[(k-1)\Delta t])/\Delta t, \quad (8)$$

where Δt is the time interval between two consecutive measurement samples indexed by k and $k-1$. For notational simplicity, we omit Δt from the sampled values, representing the sample at $t = k\Delta t$ by $x[k]$ and the previous sample by $x[k-1]$. By applying the discretization in (8) to the physics-based equation in (4) its discrete-time form is obtained as:

$$v_a[k] - v_b[k] = \frac{L_{ab}}{\Delta t}\left[\left(i_a[k] - C_a\,\frac{v_a[k]-v_a[k-1]}{\Delta t}\right) - \left(i_a[k-1] - C_a\,\frac{v_a[k-1]-v_a[k-2]}{\Delta t}\right)\right] + R_{ab}\left(i_a[k] - C_a\,\frac{v_a[k]-v_a[k-1]}{\Delta t}\right). \quad (9)$$

The problem in (7) can be expressed in discrete time as

$$\min_{\mathbf{x}[k]} \sum_k \Big[\|\mathbf{x}[k] - \mathbf{z}_v[k]\|_2^2 + \lambda\|\mathbf{E}_0\mathbf{x}[k] + \mathbf{E}_1\mathbf{x}[k-1]+ \mathbf{E}_2\mathbf{x}[k-2] - \mathbf{F}_0\mathbf{z}_i[k] - \mathbf{F}_1\mathbf{z}_i[k-1]\|_2^2\Big]. \quad (10)$$

Note that the matrices depend on the sampling interval Δt.

C. Data Quality Issues

As discussed in Section II, the high-resolution nature of waveform measurements makes SWSE more susceptible to data quality challenges. While standard measurement noise is inherently handled by the least-squares formulation in (10), other data quality issues are not directly addressed. Therefore, the formulation in (10) must be extended to handle such issues.

This leads to a fundamental principle in power system state estimation: even under full observability, where measurement units are installed at every bus, state estimation remains essential and challenging. As emphasized in the seminal work in [4] by the pioneers of PMU technology, the presence of redundant measurements is not merely a safeguard but a critical mechanism for enhancing accuracy and robustness.

Measurement errors can arise in various forms, including latched, inaccurate, or erroneous samples. Latched data malfunctions occur when the same value of $v[k]$ or $i[k]$ is recorded across multiple samples. Inaccurate data arises when a sample deviates from its expected value, for example due to loss of GPS synchronization. Erroneous data typically appears as an isolated outlier within a voltage or current sequence.

III. Solution Methodology

A. Closed-Form Solution Considering Initial Conditions

Solving problem (10) requires incorporating the *initial conditions* of the power system. Note that, at each sample k, the formulation in (10) depends on $\mathbf{x}[k-1]$ and $\mathbf{x}[k-2]$. The initial conditions can be specified as $\mathbf{x}[0] = \mathbf{d}_0$ and $\mathbf{x}[1] = \mathbf{d}_1$, which can also be expressed as a single *equality* constraint:

$$\mathbf{C}\mathbf{x} = \mathbf{D}, \quad \text{where} \quad \mathbf{x} = [\,\mathbf{x}[0]\ \mathbf{x}[1]\ \ldots\ \mathbf{x}[K]\,]. \quad (11)$$

Parameter K denotes the total number of samples.

We can combine both terms and all K samples to express the objective function in (10) in a single compact form as a function of $\mathbf{x}$. Together with the constraint in (11), the SWSE problem, with the initial conditions, can be expressed as:

$$\min_{\mathbf{x}} \ \|\mathbf{H}\mathbf{x} - \mathbf{P}\mathbf{z}\|_2^2 \quad \text{s.t.} \ \ \mathbf{C}\mathbf{x} = \mathbf{D}, \quad (12)$$

where $\mathbf{z} = [\,\mathbf{z}[1]\ \ldots\ \mathbf{z}[K]\,]$ contains all measurement samples.

We can write the Karush–Kuhn–Tucker (KKT) conditions of the above constrained convex optimization problem as follows [15, pp. 243], which is a system of linear equations:

$$\begin{bmatrix} \mathbf{H}^\top\mathbf{H} & \mathbf{C}^\top \\ \mathbf{C} & 0 \end{bmatrix}\begin{bmatrix} \mathbf{x} \\ \boldsymbol{\eta} \end{bmatrix} = \begin{bmatrix} \mathbf{H}^\top\mathbf{P}\mathbf{z} \\ \mathbf{D} \end{bmatrix}. \quad (13)$$

Let us define $\mathbf{G} = \mathbf{H}^\top \mathbf{H}$ and $\mathbf{c} = \mathbf{H}^\top \mathbf{P}\mathbf{z}$. We can obtain the following *closed-form* solution for the above KKT equations:

$$\mathbf{x}^\star = \mathbf{G}^{-1}\Big[\mathbf{c} - \mathbf{C}^\top \big(\mathbf{C}\mathbf{G}^{-1}\mathbf{C}^\top\big)^{-1}\big(\mathbf{C}\mathbf{G}^{-1}\mathbf{c} - \mathbf{D}\big)\Big]. \quad (14)$$

In case $\mathbf{G}$ is singular, $\mathbf{G}^{-1}$ is replaced with pseudoinverse.

As SWSE estimates the state at every waveform sample, the number of state variables is much larger than in traditional SE. As a result, traditional iterative solvers would be computationally burdensome and sensitive to initialization. Therefore, the closed-form solution in (14) can ensure practical scalability.

From a computational perspective, the matrices in (12)–(14) scale with the number of samples K within the estimation window. Both memory usage and computational cost grow linearly with K for a fixed network size. In real-time applications, SWSE can be implemented using a sliding-window, where only the most recent K samples are retained and older samples are dropped. Under such implementation, only the measurement vector $\mathbf{z}$ is updated as new waveform data arrive.

B. Algorithm to Enhance Robustness

In this section, we seek to enhance robustness against the various data quality issues that we discussed in Section II-C.

A common approach to improving robustness in traditional state estimation is to replace ℓ_2 norms with ℓ_1 norms, or to augment ℓ_2-based objectives with ℓ_1 regularization [16]. However, such approaches generally do not admit closed-form solutions, which is a significant limitation given the computational burden of SWSE. Moreover, while ℓ_1-based techniques can mitigate occasional and isolated outliers, they are not designed to handle issues such as time-synchronization errors or latched samples. Finally, they do not capture *temporal* consistency or inconsistency across samples and waveform cycles, which is essential in waveform analysis.

Therefore, we instead combine elements of classical statistics and robustness methods with algorithmic innovations to address the diverse data quality challenges that arise in practice. The proposed algorithm is summarized in Algorithm 1.

We start by calculating the *residual errors* in the objective function in (12), where $\mathbf{W}$ is a *diagonal weighting matrix*:

$$\mathbf{r} = \big|\mathbf{W}(\mathbf{H}\mathbf{x}^\star - \mathbf{P}\mathbf{z})\big|, \quad (15)$$

Initially, $\mathbf{W}$ is set to the identity matrix, with all diagonal entries equal to one. If data quality issues are detected, selected diagonal entries of $\mathbf{W}$ are reduced so that the corresponding terms in the objective function in (12) receive *less* weight.

To detect inconsistency in the SWSE solution, we apply a statistical approach based on the Median Absolute Deviation (MAD) to each row of vector $\mathbf{r}$. This approach is widely used as a pre-processing tool [17], whereas here we rather use it as an integrated element of our algorithm. First, we define:

$$\sigma_{\mathbf{r}} = \gamma \times \mathrm{Median}\big(|\mathbf{r} - \mathrm{Median}(\mathbf{r})|\big). \quad (16)$$

A typical value for coefficient γ is 1.4826. Let $\mathcal{O}$ denote the set of all measured samples for which the corresponding row in vector $\mathbf{r}$ satisfies the following inequality:

$$|\mathbf{r} - \mathrm{Median}(\mathbf{r})| \geq \tau\, \sigma_{\mathbf{r}}, \quad (17)$$

Algorithm 1 Robustness-Enhanced SWSE

1: Waveform Measurements: $\mathbf{z}$; Model: $(\mathbf{H}, \mathbf{P}, \mathbf{C}, \mathbf{D})$
2: Set $\delta^\star = 0$. Set $c_1 = 0$. Set $c_2 = 0$.
3: Set $\mathbf{W}$ = Identity Matrix.
4: **repeat**
5: Set $\mathbf{x}^\star$ as in (12)-(14), using $(\mathbf{WH}, \mathbf{WP})$ instead of $(\mathbf{H}, \mathbf{P})$.
6: Set Residual Vector $\mathbf{r}$ as in (15).
7: Set Outliers Matrix $\mathcal{O}$ using (16) and (17).
8: **if** $\mathcal{O} = \{\}$ **then**
9: **return** $\mathbf{x}^\star$ and $\delta^\star$
10: **else**
11: Set Counter $c_1 \leftarrow c_1 + 1$.
12: Update Matrix $\mathbf{W}$ using (18)-(20).
13: **until** $c_1 \geq C_1$
14: Set $c_2 \leftarrow c_2 + 1$
15: **if** $c_2 \geq C_2$ **then** Remove sensor n_{Issue}. Go To Line 2.
16: Set $\delta^\star = (-1)^{c_2}\lceil c_2/2 \rceil$.
17: Time-shift $\mathbf{z}$ by $\delta^\star \mathbf{q}$ samples where $\mathbf{q}$ is set as in (21).
18: Go to Line 3.

where τ is a parameter that adjusts the detection threshold. If $\mathcal{O} = \{\}$, then the SWSE results in (14) are deemed reliable, and Algorithm 1 ends. Otherwise, if $\mathcal{O} \neq \{\}$, then corrective actions are needed to address the outliers, as we discuss next.

Occasional Erroneous Measurement Samples: If set $\mathcal{O}$ contains only a few samples, the issue is likely a *momentary malfunction* in an otherwise functional sensor.

For each sample index k in set $\mathcal{O}$, a follow-up cross-examination is conducted to identify the voltage or current measurement that is likely causing the inconsistency in the SE results. In this regard, we calculate the absolute value of the difference between the measurement at sample k and the corresponding sample in the previous waveform cycle, i.e., at $k - T/\Delta t$, where T denotes the period of the fundamental component of the voltage and current waveforms [18, p. 151]:

$$\Delta z_j[k] = |z_j[k] - z_j[k - T/\Delta t]|, \quad j \in \{\mathcal{N}, \mathcal{L}\}. \quad (18)$$

If $\Delta z_j[k]$ is large, then it indicates that the measurement at node or line j at sample k experiences a large deviation from the sample in the previous cycle at the *same* WMU. For each sample k in set $\mathcal{O}$, the nodal voltage or the line current that has the largest cycle-by-cycle deviation is identified as:

$$j_k^\star = \arg \max_{j \in (\mathcal{N} \cup \mathcal{L})} |\Delta z_j[k] - \mathrm{Median}(\Delta \mathbf{z}[k])|. \quad (19)$$

After identifying $j_k^\star$ for all the samples k in set $\mathcal{O}$, the corresponding weights are updated (down-weighted) as follows:

$$\text{Multiply the Diagonal Entry in } \mathbf{W} \text{ Corresponding to Sample } k \text{ and Node or Line } j_k^\star \text{ by } \alpha, \quad (20)$$

where $0 < \alpha < 1$. Based on the above update mechanism, we repeat the process in Lines 4 to 12 in Algorithm 1 until either a solution is obtained without outliers or the maximum counter C_1 is reached. If the counter is reached, the inconsistency in the results is deemed *persistent*. In that case, a different approach needs to be triggered, as we will discuss next.

Persistent Errors Due to Issues in Time Synchronization: If residuals remain large despite applying the adjustment mechanism through matrix $\mathbf{W}$, a possible data quality issue is an error in time synchronization. In such cases, the measurement

samples from the affected WMU may still be usable, but their timestamps are incorrect due to clock drift. This results in *time-shifted* waveform samples from the impacted WMU. The goal in this step is therefore to estimate the amount of time shift and compensate for it by adjusting the timestamps of the affected sensor using an appropriate correction factor.

The pseudocode for this stage is given in Lines 14 to 18 of Algorithm 1. Note that it reaches Line 14 *only if* it does *not* return the results in Line 9 after multiple adjustments of matrix $\mathbf{W}$. Starting from $c_2 = 1$, the equation in Line 16 generates a new value for the time-shift parameter $\delta^\star$ in each execution of Lines 14 to 18. The values follow the sequence $-1, +1, -2, +2, \ldots$, representing the number of samples used to *shift* the timestamps of the measurements from the WMU suspected of experiencing time synchronization issues. The idea is to apply each shift, and then rerun the process in Lines 3 to 13 to determine whether the large residuals are resolved.

All entries in vector $\mathbf{q}$ in Line 17 that correspond to the measurements from the affected WMU are set to 1, while all other entries are set to 0. Hence, in Line 17, only the samples from the affected WMU are time-shifted by $\delta^\star$ samples.

To identify the WMU that is affected by error in time synchronization, we compare the nodal voltage of each WMU with the *simultaneous* nodal voltages in its closest neighboring WMUs. For each node $n \in \mathcal{N}$, let us define $\mathcal{M}_n \subseteq \mathcal{N}$ as the set of *two nearest nodes*. We identify the node whose WMU is the candidate for losing time synchronization as follows:

$$n_{\text{Issue}} = \arg\max_{n \in \mathcal{N}} \sum_{o \in \mathcal{M}_n} \left| \sum_k z_{v,n}[k] - z_{v,o}[k] \right|, \qquad (21)$$

Here, we do *not* include current measurements in (21), since they are not comparable in neighboring nodes for detecting time synchronization issues. See the real-world study in [19].

Once n_{Issue} is identified, it is used to construct vector $\mathbf{q}$ with corresponding 0 and 1 entries, as explained earlier.

Persistent Errors Due to Faulty Sensors: If the residuals remain high under various adjustments of matrix $\mathbf{W}$ and the time-shift parameter $\delta^\star$, the cause is likely more fundamental, such as hardware or firmware issues. In such cases, the algorithm identifies the affected WMU as faulty and removes all its measurements once the maximum counter C_2 is reached.

IV. Case Studies

The proposed robust SWSE method is evaluated on a modified IEEE 14-bus system modeled in PSCAD. The simulation time step is set to $\Delta t = 50$ μs. A solar farm [20, Article 521] is connected to bus 12 to include IBR dynamics. Data for loads, generators, transformers, power lines, and shunt capacitors are taken from [20, Article 26]. All nodal voltage waveforms and line current waveforms are measured. Noise and data quality issues are injected into the measurements to evaluate the robustness of the proposed SWSE framework.

We consider four representative events: capacitor energization at bus 9, capacitor de-energization at bus 9, IBR connection at bus 12, and IBR disconnection at bus 12.

Fig. 2 shows the performance of the proposed *closed-form* SWSE (Section III-A) compared to the noisy measurements

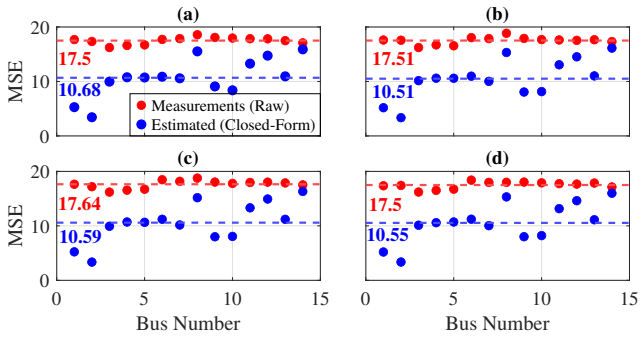

Fig. 2. Performance of the closed-form SWSE solution under 5% measurement noise, during: (a) Capacitor energization at bus 9; (b) Capacitor de-energization; (c) IBR connection at bus 12; and (d) IBR disconnection.

for all four event types. The measurement noise follows a Gaussian distribution with mean zero and variance 0.05. Each Mean Squared Error (MSE) is averaged over 100 random noise realizations, with each estimation window starting one cycle *before* and ending one cycle *after* the event. As shown in all four sub-figures, the closed-form SWSE significantly reduces the MSE by mitigating the impact of measurement noise.

While the focus of this paper is on scenarios with *full* observability, it is also insightful to briefly examine cases with *partial* observability. In such cases, the performance of the proposed method depends on the specific WMU placement. For example, under 5% measurement noise, the absence of a WMU at bus 2 is well tolerated, with estimation accuracy maintained and the MSE increasing by only 9.5%. In contrast, the absence of a WMU at bus 10 can double the MSE. A more in-depth treatment of partial observability would require a careful analysis of WMU placement, and it may also benefit from incorporating advanced techniques such as *sparse signal recovery* [21], which are both beyond the scope of this paper.

Algorithm Performance and Benchmark Comparison: We assess the performance of Algorithm 1 (Section III-B) in terms of robustness to data quality issues and compare it with both the classical ℓ_1-based method and the Huber M-estimator solved via Iteratively Reweighted Least Squares (IRLS) [22]. Huber-IRLS mitigates the impact of isolated outliers by adaptively downweighting large residuals. However, it does *not* explicitly identify the WMU responsible for the data quality issue to allow removing the malfunctioning sensor device.

For this analysis, data quality issues are introduced during the capacitor energization event at bus 9. Fig. 3(a) shows three nodal voltage waveform measurements, each containing outliers at different sample instants. Fig. 3(b) compares the performance of Algorithm 1 with the closed-form SWSE solution, the ℓ_1-based robust method, and the Huber-IRLS method. Algorithm 1 accurately estimates the voltage waveforms at all buses, whereas the ℓ_1-based and Huber-IRLS methods fail to fully mitigate the effects of multiple outliers across several buses. Figs. 3(c) and 3(d) show the initial residual terms, r_v and r_i, obtained from the closed-form solution before running Algorithm 1. Several outliers can be seen, especially in r_v.

Fig. 4(a) shows a data quality issue where the voltage waveform from one WMU is *not time-synchronized* with the measurements from the rest of the WMUs. The true voltage is in blue, and the time-misaligned voltage in red. Fig. 4(b)

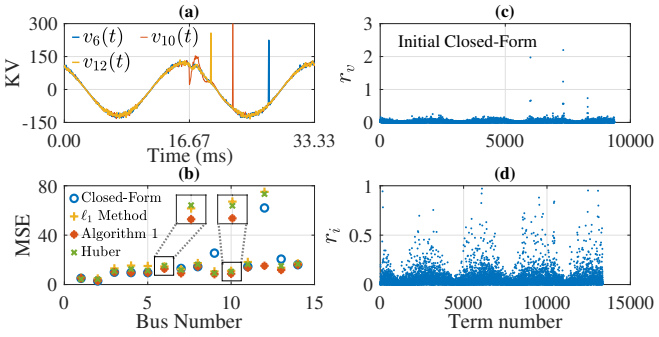

Fig. 3. Performance in the presence of sample malfunctions: (a) Voltage waveforms with multiple outliers; (b) corresponding MSE comparison across different methods; (c) and (d) Initial residual terms, r_v and r_i.

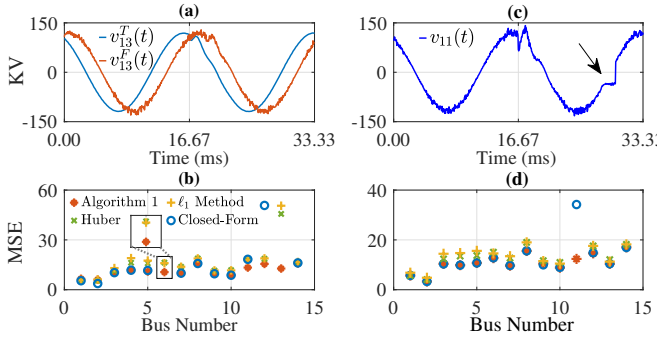

Fig. 4. (a) true (blue) and time-misaligned (red) voltages; (b) corresponding MSE comparison across different methods; (c) voltage waveform with latched samples; (d) corresponding MSE comparison across different methods.

shows that the *initial* closed-form SWSE fails to estimate the voltages at buses 13 and 6. Other method also perform poorly at bus 13, whereas Algorithm 1 estimates all states correctly.

Fig. 4(c) shows an example for a sample-latching issue. In Fig. 4(d), Algorithm 1 accurately estimates the voltage despite this malfunction, whereas the initial closed-form SWSE solution and other robust methods fail at bus 11.

1) Preliminary Parameter Sensitivity Analysis: The robustness parameters τ, α, C_1, and C_2 are selected based on practical considerations. For the outlier detection threshold τ, we adopt the commonly used value of 3 in signal processing and robust statistics; larger values (e.g., 5 and 10) yield similar performance. The parameter α, which controls outlier attenuation, was tested using values of 0.01 and 0.001 and resulted in comparable estimation accuracy. Similarly, varying C_1 over the range 3–10 had little impact on performance. The parameter C_2 defines the maximum acceptable time-synchronization error, beyond which measurements are discarded. For example, when $C_2 > 40$, the proposed method corrects the time delay of the WMU at bus 11, whereas smaller values of C_2 lead to its exclusion from the estimation problem.

V. Conclusions and Future Work

This paper introduced SWSE as a framework for continuous estimation of voltage and current waveforms across the power network. A unified continuous-time and discrete-time formulation was developed, together with a closed-form solution and a robust extension to address data quality challenges and the initial conditions. Through detailed case studies, the results showed that the proposed robust SWSE achieves accurate estimation even under severe data distortion instances.

SWSE can support a wide range of emerging applications in power systems, such as high-fidelity transient monitoring, IBR monitoring, oscillation analysis, and power quality diagnostics.

Future work can include addressing partial observability by using techniques from sparse signal recovery, as well as addressing computational complexity and real-world implementation, hardware or field data validation, and generalization of the model to different network topology configurations.

References

[1] A. S. Dobakhshari, *et al.*, "Robust hybrid linear state estimator utilizing scada and pmu measurements," *IEEE Trans. on Power Systems*, vol. 36, no. 2, pp. 1264–1273, 2021.

[2] M. Ghosal and V. Rao, "Fusion of multirate measurements for nonlinear dynamic state estimation of the power systems," *IEEE Trans. on Smart Grid*, vol. 10, no. 1, pp. 216–226, 2019.

[3] J. A. Massignan, J. B. London, *et al.*, "Bayesian inference approach for information fusion in distribution system state estimation," *IEEE Trans. on Smart Grid*, vol. 13, no. 1, pp. 526–540, 2022.

[4] A. G. Phadke and J. S. Thorp, *Synchronized phasor measurements and their applications*. Springer, 2008.

[5] I. Molina-Moreno, A. Medina, *et al.*, "Enhanced harmonic state estimation in unbalanced three-phase electrical grids based on the kalman filter and physical scale-down implementation," *International Journal of Electrical Power & Energy Systems*, vol. 123, p. 106243, 2020.

[6] P. Mack, M. de Koster, *et al.*, "Power quality state estimation for distribution grids based on physics-aware neural networks—harmonic state estimation," *Energies*, vol. 17, no. 21, p. 5452, 2024.

[7] I. Molina-Moreno *et al.*, "A methodology for transient state estimation based on numerical derivatives, optimal monitoring, filtered measurements," *IEEE Trans. on Power Delivery*, vol. 33, pp. 1527–1535, 2017.

[8] W. Xu, *et al.*, "Synchronized waveforms – a frontier of data-based power system and apparatus monitoring, protection, and control," *IEEE Trans. on Power Delivery*, vol. 37, no. 1, pp. 3–17, 2022.

[9] C. Halliday, "Visualization of real-time system dynamics using enhanced monitoring (visor)," *SP Energy Netw., Glasgow, UK, Tech. Rep*, 2018.

[10] P. G. Estevez and S. Maslennikov, "Extension of the complex dissipating energy flow method for sub/super-synchronous oscillation source location," *IEEE Trans. on Power Systems*, pp. 1–12, 2025.

[11] D. Sun, H. Liu, S. Liu, and T. Bi, "Development of synchronized waveform measurement and its application on fault detection," *IEEE Trans. on Instrumentation and Measurement*, vol. 72, pp. 1–11, 2023.

[12] H. Mohsenzadeh-Yazdi, F. Ahmadi-Gorjayi, and H. Mohsenian-Rad, "Data-driven modeling of sub-cycle dynamics of inverter-based resources using real-world synchro-waveform measurements," *IEEE Trans. on Power Delivery*, vol. 40, no. 4, pp. 2314–2326, 2025.

[13] W. Qiu, H. Yin, *et al.*, "Synchro-waveform-based event identification using multi-task time-frequency transform networks," *IEEE Trans. on Smart Grid*, vol. 16, no. 3, pp. 2647–2658, 2025.

[14] G. Miano and A. Maffucci, *Transmission lines and lumped circuits: fundamentals and applications*. Elsevier, 2001.

[15] S. P. Boyd and L. Vandenberghe, *Convex Optimization*. Cambridge University Press, 2004.

[16] V. Kekatos *et al.*, "Distributed robust power system state estimation," *IEEE Trans. on Power Systems*, vol. 28, pp. 1617–1626, 2013.

[17] G. Tang, K. Wu, J. Lei, Z. Bi, and J. Tang, "From landscape to portrait: a new approach for outlier detection in load curve data," *IEEE Trans. on Smart Grid*, vol. 5, no. 4, pp. 1764–1773, 2017.

[18] H. Mohsenian-Rad, *Smart Grid Sensors: Principles and Applications*. Cambridge University Press, UK, Apr. 2022.

[19] Z.-J. Ye and H. Mohsenian-Rad, "Transforming conventional waveform measurements into synchro-waveforms: A data-driven method for event signature alignment and synchronization operator estimation," *IEEE Trans. on Smart Grid*, vol. 16, no. 2, pp. 1495–1509, 2025.

[20] https://www.pscad.com/knowledge-base/article.

[21] K. Jiang , *et al.*, "Block-sparse bayesian learning method for fault location in active distribution networks with limited synchronized measurements," *IEEE Trans. on Power Systems*, vol. 36, no. 4, pp. 3189–3203, 2021.

[22] P. J. Huber, "Robust statistics," in *International encyclopedia of statistical science*. Springer, 2011, pp. 1248–1251.